TCP Transl Clin Pharmacol
2019;27(2):52-58
https://doi.org/10.12793/tcp.2019.27.2.52

TUTORIAL

Understanding the pharmacokinetics of reversible metabolism

Seungil Cho* and Young-Ran Yoon*

Molecular Diagnostics and Imaging Center, Kyungpook National University; Department of Molecular Medicine, School of Medicine, Kyungpook National University; Department of Clinical Pharmacology, Clinical Trial Center, Kyungpook National University Hospital, Daegu 41944, Korea

*Correspondence: S. Cho; Tel: +82-53-200-6359, Fax: +82-53-422-4950, E-mail: chosi1@gmail.com
Y-R. Yoon; Tel: +82-53-420-4950, Fax: +82-53-426-4944, E-mail: yry@knu.ac.kr

Check for updates

Received 27 May 2019
Accepted 3 Jun 2019

Keywords
Equilibrium approximation, Matrix Method, Pharmacokinetics, Reversible Metabolism, Steady-state approximation

pISSN: 2289-0882
eISSN: 2383-5427

This tutorial introduces the mathematical skills required to obtain exact and approximate solutions for reversible reactions and provides graphical insights to help understand the pharmacokinetics of reversible metabolism. The matrix method provides an easy way to derive the exact solution for the amount of each species as a function of time. The plots of the exact solutions reveal some characteristic features of the pharmacokinetic profiles of the reversible metabolism. We also describe two approximation approaches, steady-state approximation, and equilibrium approximation, to simplify the solutions. The skills and knowledge acquired through this tutorial will provide a basis for understanding more complex reversible reaction systems.

Introduction

Reversible reactions are commonly encountered in pharmacology, chemistry, biology, chemical engineering, etc.[1-6] The influence of reversible metabolism on the pharmacokinetics of a drug and its metabolites has been the subject of considerable recent research.[5-11] An interesting example is the administration of chiral drugs. Two enantiomers of a chiral drug, such as ibuprofen[10] and propranolol,[11] often have different potencies and pharmacokinetic profiles.[8-11] However, one enantiomer is usually interconverted into the other within the human body.[7-11] When a chiral drug is administered as a racemic mixture, its bioavailability and efficacy can be incorrectly estimated if reversible reactions between two enantiomers are not taken into account.[5,6] For the determination of an appropriate dosage regimen of a drug, it is therefore important to understand the characteristics of the reversible reaction between a drug and its metabolite.

In this tutorial, we focus on the basics of the pharmacokinetics of reversible metabolism. For a simple reversible reaction scheme, we use the matrix method to get exact solutions and plot them to find characteristic relationships between the pharmacokinetic profiles of a parent drug and its metabolites. In addition, we describe two approximation approaches to deal with complex problems and examine the conditions required for the successful application of each approach.

Copyright © 2019 Seungil Cho and Young-Ran Yoon
It is identical to the Creative Commons Attribution Non-Commercial License (http://creativecommons.org/licenses/by-nc/3.0/).
This paper meets the requirement of KS X ISO 9706, ISO 9706-1994 and ANSI/NISO Z.39.48-1992 (Permanence of Paper).

Reviewer
This article was invited and reviewed by the peer experts who are not TCP editors.

Theoretical analysis

Exact solution for the kinetics of reversible reaction

Let us consider the following simple reversible reaction scheme

$$A \underset{k_2}{\overset{k_1}{\rightleftarrows}} B \xrightarrow{k_3} C,$$

Where the first step is reversible with a forward rate constant k_1 and reverse rate constant k_2, and the second step is irreversible with the rate constant k_3. The rate constant has the units of the amount per unit time, which are omitted for simplicity in this tutorial. The rate equations are:

$$\frac{dA}{dt} = -k_1 A + k_2 B \quad (1)$$

$$\frac{dB}{dt} = k_1 A - (k_2 + k_3) B \quad (2)$$

$$\frac{dC}{dt} = k_3 B \quad (3)$$

Linear ordinary differential equations can be solved using Laplace transformation or the matrix method.[2,3,7,12] We used the latter to obtain an exact solution because of its simplicity. The above expressions can be written in matrix form:

$$M = \begin{bmatrix} -k_1 & k_2 & 0 \\ k_1 & -(k_2 + k_3) & 0 \\ 0 & k_3 & 0 \end{bmatrix} \quad (4)$$

By setting $\begin{vmatrix} -k_1 - \lambda & k_2 & 0 \\ k_1 & -(k_2 + k_3) - \lambda & 0 \\ 0 & k_3 & -\lambda \end{vmatrix} = 0$, where λ is the eigenvalue, and solving for λ, we get the following characteristic polynomial:

$$\lambda(\lambda^2 + p\lambda + q) = 0 \quad (5)$$

Where $p = k_1 + k_2 + k_3$ and $q = k_1k_3$. The solutions of the quadratic equation in Eq. (5) are given by

$$\alpha = \frac{p+\sqrt{p^2-4q}}{2},$$

and

$$\beta = \frac{p-\sqrt{p^2-4q}}{2}.$$

The resulting eigenvalues are 0, -α, and -β. These eigenvalues are substituted into the eigenvalue equation to yield the corresponding eigenvectors of

$\begin{bmatrix} 0 \\ 0 \\ 1 \end{bmatrix}$, $\begin{bmatrix} \beta - k_1 \\ k_1 \\ \beta \end{bmatrix}$, and $\begin{bmatrix} \alpha - k_1 \\ k_1 \\ \alpha \end{bmatrix}$, spectively.

Because the matrix M has three distinct real eigenvalues and their corresponding eigenvectors, we can express the solution as

$$\begin{bmatrix} A \\ B \\ C \end{bmatrix} = C_0 \begin{bmatrix} 0 \\ 0 \\ 1 \end{bmatrix} + C_1 \begin{bmatrix} \beta - k_1 \\ k_1 \\ \beta \end{bmatrix} e^{-\alpha t} + C_2 \begin{bmatrix} \alpha - k_1 \\ k_1 \\ \alpha \end{bmatrix} e^{-\beta t} \quad (6)$$

At $t = 0$, $A = A_0$ and $B = C = 0$, and $A + B + C = A_0$ at all times. Using these boundary conditions, we can solve Eq. (6) to get $C_0 = A_0$, $C_1 = -C2$ and $C_1 = A_0/(\beta - \alpha)$. Then, the final expressions for the above differential equations (1–3) are

$$A = \frac{A_0}{\beta-\alpha}\{(\beta - k_1)e^{-\alpha t} - (\alpha - k_1)e^{-\beta t}\} \quad (7)$$

$$B = \frac{k_1 A_0}{\beta-\alpha}\left(e^{-\alpha t} - e^{-\beta t}\right) \quad (8)$$

$$C = \frac{A_0}{\beta-\alpha}\left(\beta - \alpha + \alpha e^{-\beta t} - \beta e^{-\alpha t}\right) \quad (9)$$

We can compare these results to those for a consecutive two-step reaction, as described in the previous tutorial.[13] We can easily show that the latter has the eigenvalues of 0, $-k_1$, and $-k_3$, by setting $k_2 = 0$ in Eq. (5). The solutions for *B* and *C*, equations 8 and 9 in this study, are very similar to those for the consecutive reaction (Equations 7 and 9 in Reference,[13] respectively). Thus, the expressions for the maximum amount of *B* (B_{max}) and the time to reach the peak (t_{max}) can be obtained in a similar way:

$$t_{max} = \frac{1}{\beta-\alpha}\ln\frac{\beta}{\alpha} \quad (10)$$

and

$$B_{max} = A_0 \frac{k_1}{\beta}\left(\frac{\alpha}{\beta}\right)^{\frac{\alpha}{\beta-\alpha}} = A_0 \frac{k_1}{\alpha}\left(\frac{\alpha}{\beta}\right)^{\frac{\beta}{\beta-\alpha}}, \quad (11)$$

respectively.

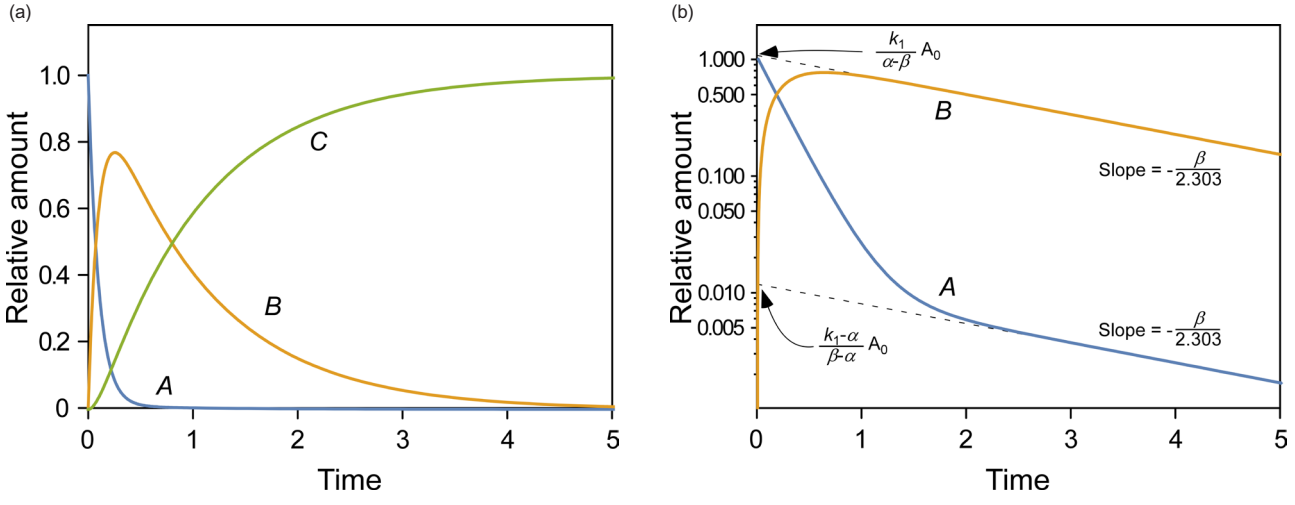

Figure 1. (a) Linear and (b) semi-logarithmic plots of the amount-time curves of *A*, *B*, or *C* in the reversible reaction, $A \underset{k_2}{\overset{k_1}{\rightleftarrows}} B \xrightarrow{k_3} C$, where $k_1 = 10$, $k_2 = 0.1$, and $k_3 = 1$. The abscissa and ordinate denote the time and the amount of each species, respectively, in arbitrary unit. See text for details.

Graphical insights into the kinetics of reversible reactions

Figure 1 shows representative amount versus time curves of *A*, *B*, and *C*, plotted on a linear and semi-logarithmic scale for three different cases: (a) $k_1 = 10$, $k_2 = 0.1$, and $k_3 = 1$; (b) $k_1 = 5$, $k_2 = 4$, and $k_3 = 2$; (c) $k_1 = 1$, $k_2 = 5$, and $k_3 = 0.2$. When k_1 and k_3 are relatively larger than k_2, that is, the reverse reaction is negligible, linear plots of the amount versus time curves of *A* and *B* for the reversible reaction (Fig. 1a) look very similar to those for a consecutive irreversible reaction (see Figure 2 in Reference[13]). The semi-logarithmic plots for the former case (Fig. 1b), however, look different from those for the latter case (see Figure 3a in Reference[13]). In the former case, two curves are always parallel to each other in the elimination phase, whereas they are not in the latter case. The difference can be explained as follows. For an irreversible reaction, the amount of *A* is described by one exponential term, whereas for the reversible reaction, it is described by two exponential terms. For the latter, the first term in Eq. (7) or (8) decreases faster than the second term over time, because α is always larger than β. This means that the elimination phase is governed by the second term. Therefore, the first term can be neglected when t is sufficiently large. In semi-logarithmic plots of *A* and *B*, thus, both slopes for the elimination phase are linear and identical and given by $-\beta/2.303$. The y-intercepts for *A* and *B* are $\frac{\alpha-k_1}{\alpha-\beta}A_0$ and $\frac{k_1}{\alpha-\beta}A_0$, respectively. When $2k_1 = 2k_2 + k_3$, the intercepts are the same, as shown in

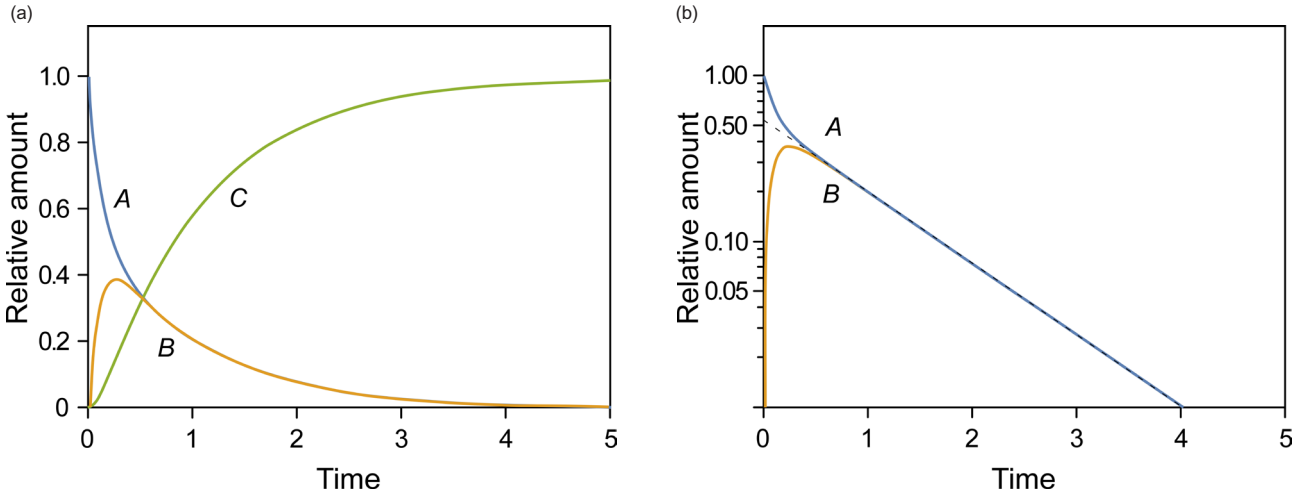

Figure 2. (a) Linear and (b) semi-logarithmic plots of the amount-time curves of *A*, *B*, or *C* in the reversible reaction, $A \underset{k_2}{\overset{k_1}{\rightleftarrows}} B \xrightarrow{k_3} C$, where $k_1 = 5$, $k_2 = 4$, and $k_3 = 2$. The abscissa and ordinate denote time and the amount of each species, respectively, in arbitrary unit. See text for details.

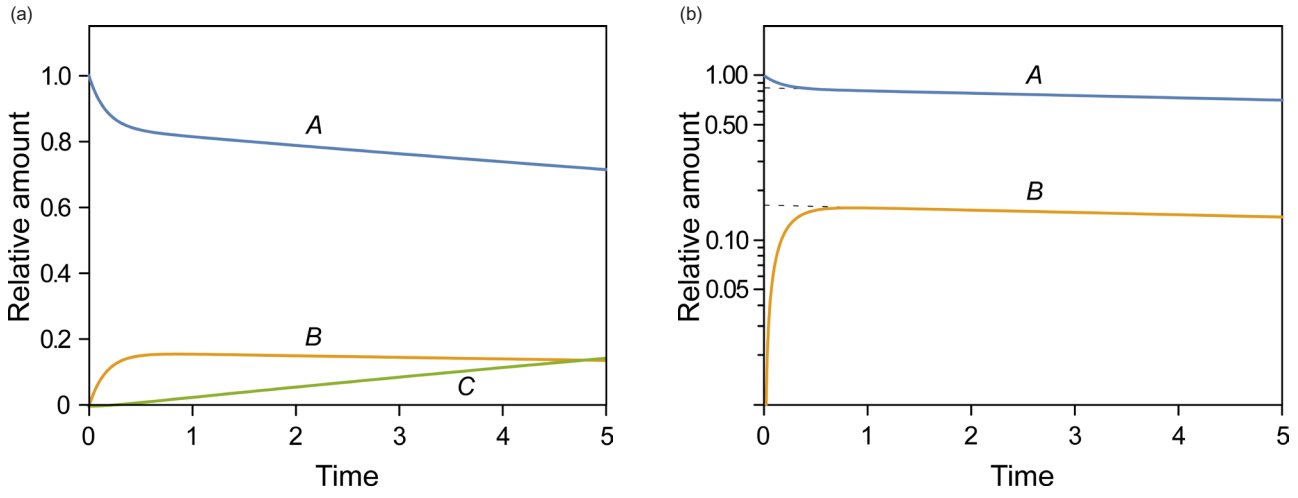

Figure 3. (a) Linear and (b) semi-logarithmic plots of the amount-time curves of *A*, *B*, or *C* in the reversible reaction, $A \underset{k_2}{\overset{k_1}{\rightleftarrows}} B \xrightarrow{k_3} C$, where $k_1 = 1$, $k_2 = 5$, and $k_3 = 0.2$. The abscissa and ordinate denote time and the amount of each species, respectively, in arbitrary unit. See text for details.

Figure 2. If $2k_1 < 2k_2 + k_3$, the curves *A* and *B* will not cross each other. As a third case, we set $k_1 = 1$, $k_2 = 5$, and $k_3 = 0.2$, which satisfies this condition. It is noteworthy that the semi-logarithmic plots for this case (Fig. 3b) strongly resemble those for the consecutive irreversible reaction (see Figure 3b in Reference[13]). In the latter case, the semi-logarithmic plots of plasma concentrations versus time of A and B become parallel straight lines at large *t* only when the formation rate of B is much slower than its elimination rate; that is, the metabolism is formation rate-limited (FRL).[13-15] In addition, the intercept for [B] becomes greater than that for [A] when the distribution volume of *B*, V_B, is much smaller than that of *A*, V_A (see Figure 3c in Reference[13]). However, we need to be cautious when we apply this feature to the interpretation of the time profiles of the semi-logarithmic plots of a drug and its metabolite because this feature is commonly observed in reversible metabolic reactions. The pharmacokinetic parameters for each case, including t_{max} and B_{max}, are summarized in Table 1.

The area under the curve (AUC) is an important pharmacokinetic parameter, representing total drug exposure over time. The AUC for *A* and *B* can be obtained by directly integrating Eqs. (7) and (8) from zero to infinity, respectively, and expressed as

$$AUC_A = \frac{(k_2+k_3)A_0}{q} \text{ and} \tag{12}$$

$$AUC_B = \frac{k_1 A_0}{q}. \tag{13}$$

Thus, the ratio of AUC_A to AUC_B can be simplified to $\frac{k_2+k_3}{k_1}$. The AUC for C can also be calculated by integrating Eq. (9) from zero to *t* and given by

$$AUC_C = A_0\left(t - \frac{p}{q}\right). \tag{14}$$

Using a time integration method,[14,16] we can obtain the relationship between AUC and rate constant or clearance, which has the units of volume (V) per unit time (CL = $k \times$ V). By separating the variables in Eqs. (7–9) and integrating both sides with respect to their respective variables, we can write the equations as follows:

$$V_A \int_{[A]_0}^{\infty} d[A] = -k_1 V_A \int_0^{\infty} [A]\, dt + k_2 V_B \int_0^{\infty} [B]\, dt, \tag{15}$$

$$V_B \int_{[B]_0}^{\infty} d[B] = k_1 V_A \int_0^{\infty} [A]\, dt - (k_2 + k_3) V_B \int_0^{\infty} [B]\, dt, \tag{16}$$

$$V_C \int_{[C]_0}^{\infty} d[C] = k_3 V_B \int_0^{\infty} [B]\, dt. \tag{17}$$

They should satisfy the following boundary conditions: [*B*] = [*C*] = 0 at t = 0; [*A*] = [*B*] = 0 and $V_C \times [C] = A_0$ at $t = \infty$. By substituting $k_1 = CL_1/V_A$, $k_2 = CL_2/V_B$, and $k_3 = CL_3/V_C$, we get

$$A_0 = CL_1 AUC_A - CL_2 AUC_B, \tag{18}$$

$$CL_1 AUC_A = (CL_2 + CL_3) AUC_B \tag{19}$$

$$A_0 = CL_3 AUC_B \tag{20}$$

Eq. (19) can be rearranged as

$$\frac{AUC_B}{AUC_A} = \frac{CL_1}{CL_2 + CL_3}. \tag{21}$$

These relationships are helpful in understanding pharmacokinetic features and metabolic pathways.[14,17,18]

Approximation of the kinetics of reversible reactions

To get a good approximate solution for a reversible reaction scheme, approximation approaches have been developed and are widely used.[12,19,20] Depending upon the reactivity of the intermediate species, we can use either of two approximation approaches. One is a steady-state approximation, in which the intermediate species *B* is very reactive and hence short lived. This approximation is useful for explaining reactions involving radical species. The other is an equilibrium approximation, in which B is quite stable and long-lived because the equilibrium reaction proceeds faster than the product formation reaction;

Table 1. Pharmacokinetic parameters for the following cases: (a) $k_1 = 10$, $k_2 = 0.1$, and $k_3 = 1$ (as in Fig. 1); (b) $k_1 = 5$, $k_2 = 4$, and $k_3 = 2$ (as in Figure 2); (c) $k_1 = 1$, $k_2 = 5$, and $k_3 = 0.2$ (as in Figure 3); (d) $k_1 = 0.1$, $k_2 = 1$, and $k_3 = 5$, (as in Figure 4a); (e) $k_1 = 10$, $k_2 = 1$, and $k_3 = 0.1$ (as in Figure 4b)

	(a)	(b)	(c)	(d)	(e)
t_{max} (*B*)	0.245	0.256	0.855	0.722	0.439
B_{max}	0.768	0.387	0.158	0.0157	0.873
$AUC_{0-\infty}$ (*A*)	0.11	0.6	26	12.0	1.1
$AUC_{0-\infty}$ (*B*)	1.00	0.5	5	0.2	10.0
AUC_{0-100} (*C*)	98.89	98.9	69	87.8	88.9
Intercept (*A*)*	0.0122	0.556	0.842	0.998	0.0924
Intercept (*B*)*	1.10	0.556	0.163	0.0169	0.915
Slope (*A* & *B*)*	0.429	0.434	0.014	0.0361	0.0394

$AUC_{0-\infty}$ and AUC_{0-100} represent the areas under the curve from $t = 0$ to $t = \infty$ and 100, respectively. All the intercepts and slopes (*) were obtained from semi-logarithmic plots.

that is, k_1, k_2 >> k_3. For both approaches, the following condition should be satisfied:

$$\frac{\mathrm{dB}}{dt} \approx 0 \tag{22}$$

In the steady-state approximation, B is extremely unstable and very short-lived and thus is present in most of the time in extremely small amounts. By assuming that $B \approx 0$, we can get a new boundary condition: $A + C = A_0$. From Eq. (22), Eq. (2) can be rearranged to yield:

$$\frac{\mathrm{B}}{A} = \frac{k_1}{k_2+k_3} \ll 1 \tag{23}$$

For the steady-state approximation, this ratio should be very small because the amount of B is much smaller than that of A. Substituting Eq. (23) into Eq. (1) and re-arranging it for A, we have

$$\frac{dA}{dt} = -\frac{k_1 k_3}{k_2+k_3} A \tag{24}$$

By separating the variables and integrating the resulting equation, we get

$$A = A_0 e^{-\frac{k_1 k_3}{k_2+k_3} t} \tag{25}$$

Using the above expression and the new boundary condition, $A + C = A_0$, we obtain

$$C = A_0 \left(1 - e^{-\frac{k_1 k_3}{k_2+k_3} t}\right) \tag{26}$$

Now we can solve Eq. (2) for B using Eq. (26), to get

$$B = A_0 \frac{k_1}{k_2+k_3} e^{-\frac{k_1 k_3}{k_2+k_3} t} \tag{27}$$

We plot the exact and approximate solutions for the case where $k_1 = 0.1$, $k_2 = 1$, and $k_3 = 5$ (Fig. 4a). Because $\frac{k_1}{k_2+k_3} = \frac{0.1}{1+5} \sim 0.017 << 1$, the requirement for the steady-state approximation is satisfied. As the reaction begins, the amount of B quickly increases but is still extremely small ($B_{max} = 0.016$ at $t_{max} = 0.72$) for most of the time, as expected. As shown in Figure 4a, the approximate solutions (dashed lines) agree well with the exact solutions (solid lines).

For the equilibrium approximation, the reaction needs to be in pseudo-equilibrium. In such a case, we can express

$$\mathrm{B} = K_{eq} A = \frac{k_1}{k_2} A, \tag{28}$$

Where K_{eq} is an equilibrium constant. Because

$$\frac{dA}{dt} + \frac{dB}{dt} + \frac{dC}{dt} = 0, \tag{29}$$

we also have

$$\frac{\mathrm{dA}}{dt} \approx 0 \text{ or } \frac{\mathrm{dC}}{dt} \approx 0.$$

Because of the above condition, it is not feasible to directly solve Eqs. (1) and (2). Instead, we need to combine the two equations to get

$$\frac{d(A+B)}{dt} = -k_3 B. \tag{30}$$

If we define $X = A + B = A_0 - C$, from Eq. (28), we can express A and B as

$$\mathrm{A} = \frac{k_2}{k_1+k_2} X \text{ and } \mathrm{B} = \frac{k_1}{k_1+k_2} X. \tag{31}$$

Now Eq. (30) can be solved for X to get

$$\mathrm{X} = A_0 e^{-\frac{k_1 k_3}{k_1+k_2} t} \tag{32}$$

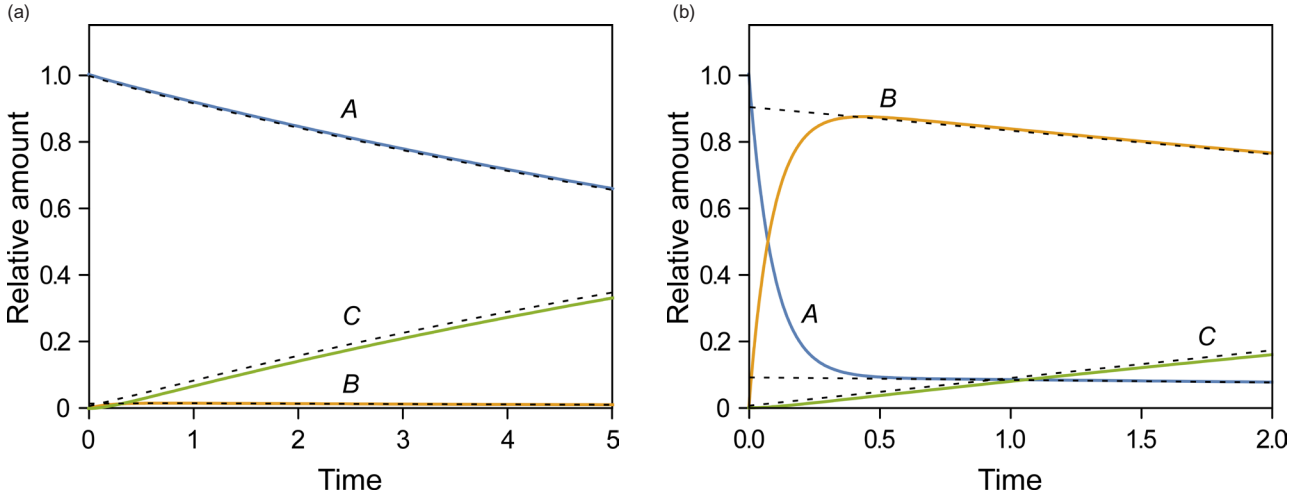

Figure 4. Linear plots of the amount-time curves of A, B, or C for the cases of (a) $k_1 = 0.1$, $k_2 = 1$, and $k_3 = 5$, corresponding to the steady-state approximation, and (b) $k_1 = 10$, $k_2 = 1$, and $k_3 = 0.1$, corresponding to the equilibrium approximation. The solid and dashed lines represent the exact and approximate solutions, respectively. The abscissa and ordinate denote time and the amount of each species, respectively, in arbitrary unit. See text for details.

Then, we have

$$A = A_0 \frac{k_2}{k_1+k_2} e^{-\frac{k_1 k_3}{k_1+k_2}t}, \quad (33)$$

$$B = A_0 \frac{k_1}{k_1+k_2} e^{-\frac{k_1 k_3}{k_1+k_2}t}, \quad (34)$$

$$C = A_0(1 - e^{-\frac{k_1 k_3}{k_1+k_2}t}). \quad (35)$$

In Figure 4b, we show the plots of the exact and approximate solutions for the case where $k_1 = 10$, $k_2 = 1$, and $k_3 = 0.1$. Unlike in Figure 4a, the amount of B is not negligible ($B_{max} = 0.87$ at $t_{max} = 0.44$). The reaction rapidly reaches quasi-equilibrium, after which the amount of B slowly decreases. As shown in Figure 4b, the approximate solutions (dashed lines) agree well with the exact solutions (solid lines).

The difference between steady-state and equilibrium approximate approaches lies in the range of their applicability.[20] When we introduce an additional constraint, $k_2 >> k_1$ into the equilibrium approach and $k_2 >> k_3$ into the steady state approach, both methods will yield the same solution.[20] This relationship can be further explained by considering an approximate expression for β. Using the following binomial theorem

$$(1+x)^n = 1 + \frac{nx}{1!} + \frac{n(n-1)x^2}{2!} + \cdots,$$

we can obtain the binomial expansion of β, which yields

$$\beta = \frac{k_1+k_2+k_3-\sqrt{(k_1+k_2+k_3)^2-4k_1k_3}}{2} = \frac{k_1k_3}{k_1+k_2+k_3} + \frac{(k_1k_3)^2}{(k_1+k_2+k_3)^3} + \frac{2(k_1k_3)^3}{(k_1+k_2+k_3)^5} + \cdots. \quad (36)$$

If $k_1 + k_2 >> k_3$ or $k_2 + k_3 >> k_1$, the second and higher order terms in the expansion can be negligible, and the first term can be further simplified to be the same as the exponent in the equilibrium approximation [see Eqs. (33-35)] or in the steady-state approximation [see Eqs. (25-27)], respectively. For a refined approximation, we can differentiate Eq. (23) for A and B with respect to time t to get

$$\frac{dB}{dt} = \frac{k_1}{k_2+k_3}\frac{dA}{dt} \quad (37)$$

By substituting Eqs. (3), (23), and (37) into Eq. (29) and rearranging the resulting equation, we get

$$\frac{dA}{dt} = -\frac{k_1k_3}{k_1+k_2+k_3}A \quad (38)$$

We expect a better approximate solution from the above equation compared with that produced by Eq. (24).

Application of the Reversible Reaction Scheme

The reversible reaction scheme is also used to describe drug distribution after rapid intravenous injection. Drug distribution within the body is often described by a two-compartment model with central and peripheral compartments.[21] In this model, an injected drug will be either eliminated or distributed within the central compartment, representing intravascular space, and the peripheral compartment, representing non-metabolizing body tissues. The distribution phase can be expressed by two linear differential equations similar to Eqs. 1 and 2.[21] The solution for drug concentration in each compartment can be obtained using a similar approach and described by two exponential terms.

To explain the kinetics of an enzyme-catalyzed reaction, a Michaelis-Menten model has been widely used.[22-24] When an enzyme and a substrate form a complex, the binding of the substrate to the active site of the enzyme is non-covalent and reversible. If the conversion of the enzyme-substrate complex to a product is the rate-limiting process, the concentration of the complex can be considered to be constant. Then, the equilibrium approximation will give a hyperbolic relationship between the initial reaction rate, v_0, and substrate concentration [S], known as the Michaelis-Menten equation,

$$v_0 = \frac{V_{max}[S]}{K_S(or\ K_m) + [S]}$$

Where V_{max} is the maximum reaction rate achieved when all of the active sites are occupied by substrates. The Michaelis constant, in the original article,[22,23] is given by $K_S = \frac{k_2}{k_1}$. When a steady-state approximation is used, the constant is given by $K_m = \frac{k_2+k_3}{k_1}$.[24]

Concluding remarks

We have described the mathematical approaches needed to determine the reaction kinetics of a reversible reaction system and provided graphical insights into the results. The knowledge acquired through this tutorial may help deepen the understanding of the pharmacokinetics of reversible metabolism and ultimately help with the prediction of the appropriate dose of a drug that is subject to equilibrium in a human body.

Acknowledgments

This study was supported by a grant of the Korean Health Technology R&D Project, Ministry of Health & Welfare, Republic of Korea (HI14C2750), as well as by the Industrial Core Technology Development Program (10051129, Development of the system for ADME assessment using radiolabeled compounds) funded by the Ministry of Trade, Industry & Energy (MOTIE, Korea).

Conflict of interest

- Authors: The authors have no conflicts of interest to declare.
- Reviewers: Nothing to declare
- Editors: Nothing to declare

References

1. Lowry TM, John WT. CCLXIX. Studies of dynamic isomerism. Part XII. The equations for two consecutive unimolecular changes. J Chem Soc Trans 1910;97:2634-2645. doi: 10.1039/CT9109702634.
2. Chrastil J. Determination of the first-order consecutive reversible reaction kinetics. Comput Chem 1993;17:103-106. doi:10.1016/0097-8485(93)80035-C.
3. Binti Hasan NAS, Balasubramanian P. Exact Solution for the Kinetic Equations of First Order Reversible Reaction Systems through Flow Graph Theory Approach. Ind Eng Chem Res 2013;52:10594-10600. doi: 10.1021/ie303501t.
4. DiStefano JJ 3rd. Concepts, properties, measurements, and computation of clearance rates of hormones and other substances in biological systems. Ann Biomed Eng 1976;4:302-319.
5. Hwang S, Kwan KC, Albert KS. A linear mode of reversible metabolism and its application to bioavailability assessment. J Pharmacokinet Biopharm 1981;9:693-709.
6. Cheng H, Jusko WJ. Pharmacokinetics of reversible metabolic systems. Biopharm Drug Dispos 1993;14:721-766.
7. Hallak HO, Wedlund PJ. Reversible metabolism of vitamin K-vitamin K epoxide: modeling considerations and limitations. J Pharmacokinet Biopharm 1992;20:1-18.
8. Eriksson T, Björkman S, Roth B, Höglund P. Intravenous formulations of the enantiomers of thalidomide: pharmacokinetic and initial pharmacodynamic characterization in man. J Pharm Pharmacol 2000;52:807-817.
9. Ebling WF, Jusko WJ. The determination of essential clearance, volume, and residence time parameters of recirculating metabolic systems: the reversible metabolism of methylprednisolone and methylprednisone in rabbits. J Pharmacokinet Biopharm 1986;14:557-599.
10. Baillie TA, Adams WJ, Kaiser DG, Olanoff LS, Halstead GW, Harpootlian H, et al. Mechanistic studies of the metabolic chiral inversion of (R)-ibuprofen in humans. J Pharmacol Exp Ther 1989;249:517-523.
11. Stoschitzky K, Lindner W, Egginger G, Brunner F, Obermayer-Pietsch B, Passath A, et al. Racemic (R,S)-propranolol versus half-dosed optically pure (S)-propranolol in humans at steady state: Hemodynamic effects, plasma concentrations, and influence on thyroid hormone levels. Clin Pharmacol Ther 1992;51:445-453.
12. Volk L, Richardson W, Lau KH, Hall M, Lin SH. Steady state and equilibrium approximations in reaction kinetics. J Chem Educ 1977;54:95-97. doi: 10.1021/ed054p95.
13. Cho S, Yoon YR. Understanding the pharmacokinetics of prodrug and metabolite. Transl Clin Pharmacol 2018;26:1-5. doi: 10.12793/tcp.2018.26.1.
14. Rowland M, Tozer TN. Clinical pharmacokinetics and pharmacodynamics: concepts and applications, 4th ed. Wolters Kluwer Health/Lippincott William & Wilkins, Philadelphia, 2011; 603-632.
15. Smith PC. Pharmacokinetics of drug metabolites. In: Pearson PG, Wienkers LC (Eds.) Handbook of drug metabolism, 2nd ed. Informa Healthcare, New York, 2009;17-59.
16. Mucientes AE, de la Peña MA. Kinetic Analysis of Parallel-Consecutive First-Order Reactions with a Reversible Step: Concentration–Time Integrals Method. J Chem Educ 2009;86:390-392. doi: 10.1021/ed086p390.
17. Pang KS. A review of metabolite kinetics. J Pharmacokinet Biopharm 1985;13:633-662.
18. de Campos ML, Padilha EC, Peccinini RG. A review of pharmacokinetic parameters of metabolites and prodrugs. Drug Metab Lett 2014;7:105-116.
19. McDaniel DH, Smoot CR. Approximations in the kinetics of consecutive reactions. J Phys Chem 1956;60:966-969. doi: 10.1021/j150541a035.
20. Pyun CW. Steady-state and equilibrium approximations in chemical kinetics. J Chem Educ 1971;48:194-196. doi: 10.1021/ed048p194.
21. Atkinson Jr AJ. Compartment analysis of drug distribution. In: Atkinson AJ, Huang S-M, Lertora JJL, Markey SP. (Eds.) Principles of Clinical Pharmacology, 3rd ed. Academic Press, Amsterdam, 2012; 27-39.
22. Michaelis L, Menten ML. Die Kinetik der Invertinwirkung. Biochem Z 1913;49:333-369.
23. Michaelis L, Menten ML, Johnson KA, Goody RS. The Original Michaelis Constant: Translation of the 1913 Michaelis–Menten Paper. Biochemistry 2011;50:8264-8269. doi: 10.1021/bi201284u.
24. Briggs GE, Haldane JB. A note on the kinetics of enzyme action. Biochem J 1925;19:338-339.